Reprinted from
"1961 Transactions of the Eighth Vacuum Symposium
and Second International Congress"
PERGAMON PRESS
OXFORD · LONDON · NEW YORK · PARIS
1962

A Magnetically Suspended Molecular Pump†

By C. E. WILLIAMS and J. W. BEAMS

University of Virginia, Department of Physics, Charlottesville, Virginia, U.S.A.

The alloy steel rotor of a bakeable molecular pump is magnetically suspended inside a stainless steel vacuum chamber and spun by a rotating magnetic field. Operational data will be given which includes ratios of the pressure on the high side to the low side of the pump as a function of rotor speed and clearance between rotor and stator. Pumping speeds of the order of 10 l./sec, pressures of 4×10^{-10} *Torr, and pressure ratios of* 10^5 *have been obtained. The experimental data will be compared with a theory worked out for the pump.*

1. Introduction

THE use of the molecular pumps for producing vacua has been amply demonstrated by many investigators[1, 2, 3, 4] and some of these pumps have been commercially available in Europe for several years. However, their design requires lubricated bearings inside the vacuum system, which render them unbakeable. As a result, they are not suited for producing an ultra high vacuum. Recently it has been possible to eliminate all bearings and lubricants inside the vacuum system by magnetically suspending the rotating parts.[5, 6] This makes the pump completely bakeable and hence useful for producing very high vacua. The purpose of this paper is to report further development of this type of molecular pump together with operational data.

In a molecular pump the pumping action is produced by the motion of one surface over another when the clearance between them is small. In these particular experiments an auxiliary pump is used to reduce the forepressure until the mean free path of the molecules is smaller than the clearance between the moving (rotating) and stationary surfaces. The moving surface is a rotor with its plane disc surface spinning a small distance below or above a stationary plane surface.

If molecules strike a polycrystalline moving surface the momentum exchange is such that they emerge from the surface with practically a random velocity distribution with respect to the moving surface. As a result, the molecules are given a resultant velocity in the direction of motion of the surface. Consequently, if channels are cut in the stator in the proper way the flow of molecules is directed along these channels and pumping action can be produced.

2. General design

The pump assembly consists of a rotor, stator, pressure gauges, and the chamber. The rotor and stator are

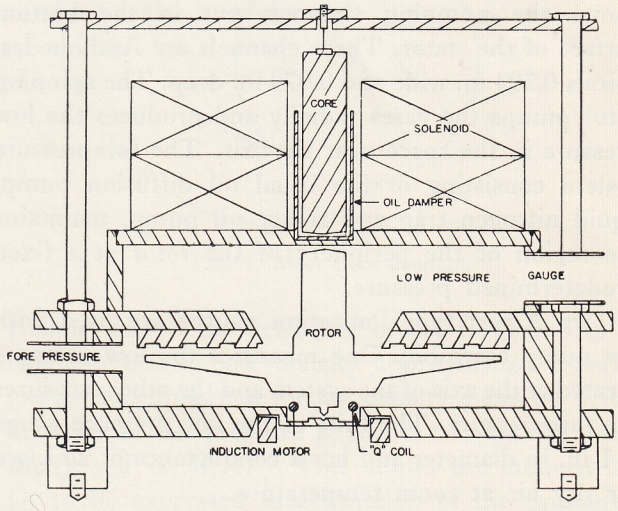

FIG. 1. Schematic diagram of magnetically suspended molecular pump.

sealed inside the chamber in their operational position, as shown in Fig. 1. The rotor is magnetically suspended by the axial magnetic field of the solenoid.

† Supported by the Navy Bureau of Weapons and by Army Research Office.

[1] W. GAEDE, *Ann. Physik* **41**, 337 (1913).
[2] F. HOLWECK, *C. R. Acad. Sci. Paris* **117**, 43 (1923).
[3] M. SIEGBAHN, *Arch. Math. Astr. Fys.* **30B**, No. 2 (1943).
[4] S. VON FRIESEN, *Rev. Sci. Instrum.* **11**, 362 (1940).
[5] J. W. BEAMS, *Science* **130**, 1406 (1959).
[6] J. W. BEAMS, *Vacuum Symposium Transactions*, p. 1 (1960) Pergamon Press, London.

It is driven by an induction motor located outside and below the chamber. A detailed description of the magnetic support system and the drive system has been reported previously.[7] The pumping action occurs between the top surface of the rotor and the bottom surface of the stator. Figure 2 is a photograph of the rotor and the stator.

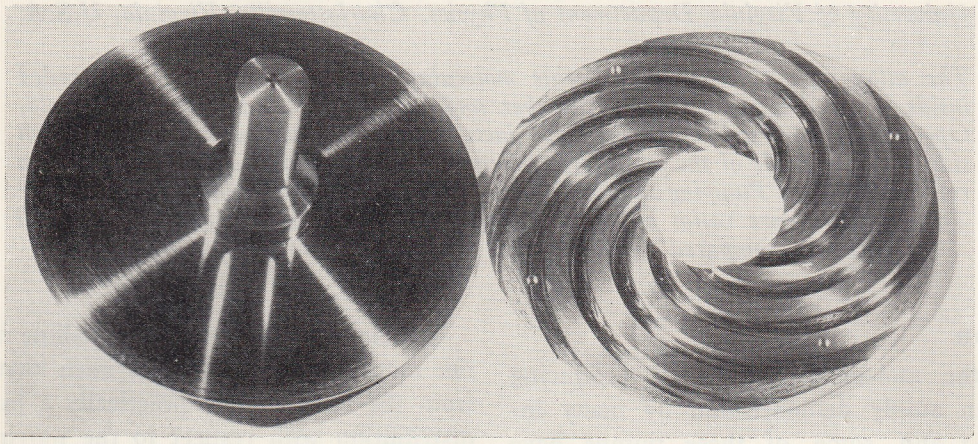

FIG. 2. Photograph of rotor and stator.

The rotor weighs 10 lb, is 9 in. in diameter and is machined from cold rolled steel. The long neck portion is for ease of adjustment and to make possible a pumping connection of large conductance. The stator is machined from aluminum or stainless steel and is 9 in. in diameter. The photograph, Fig. 2, shows the pumping channels cut in the bottom surface of the stator. These channels are Archimedes' spirals 0.394 in. wide and 0.079 in. deep. The spinning rotor pumps the gases radially and produces the low pressure in the space near the axis. The forepressure system consisting of the usual oil diffusion pump, liquid nitrogen trap and rotary oil pump, maintains the region of the periphery of the rotor at a fixed predetermined pressure.

Two Alpert type ionization gauges are used with the pump assembly. One measures the low pressure created at the axis of the system and the other measures the forepressure. The tube of the low pressure gauge is 1 in. in diameter and has a conductance of 20 l./sec for dry air at room temperature.

The chamber, shown in Fig. 1, is constructed of type 304 nonmagnetic stainless steel. The thickness of the chamber wall is 3/16 in. directly under the iron core and over the induction motor and varies to 5/8 in. for the side wall and bottom plate. The chamber is sealed by a pair of torque joints. Aluminum ring seals are compressed by sixteen 1/2 in. bolts. All the joints on the low pressure side of the chamber are heli-arc welded. For these tests the only outlet on this side of the chamber is to the low pressure ionization gauge. The gauge is sealed to the chamber at this point by a commercial glass-to-metal seal.

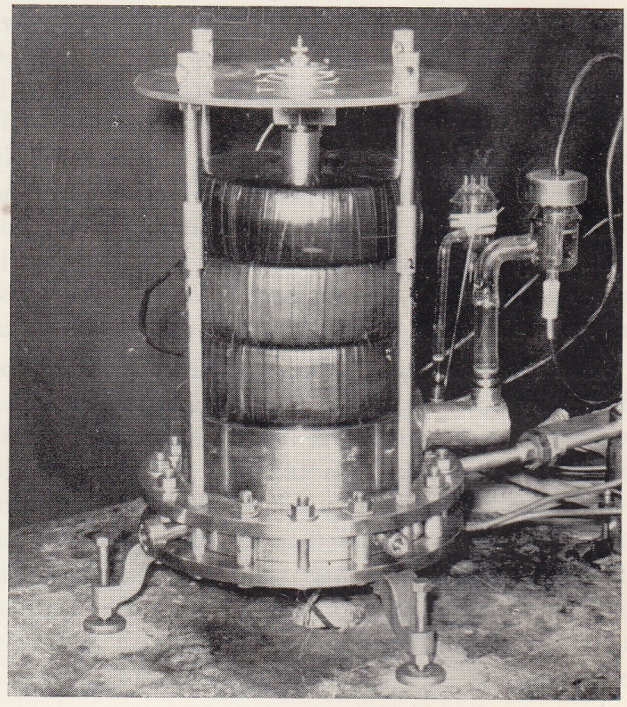

FIG. 3. Photograph of complete pumping system.

Figure 3 is a photograph of the pump as it appears completely assembled, while Fig. 4 is a photograph of the pump assembly as it looks prepared for baking.

[7] J. W. BEAMS, *Science*, **120**, 619 (1954).

Note that the rotor is not spinning and the solenoid has been removed. This is not necessary if the insulation on the solenoid windings are resistant to temperatures of 400°C since the curie point of steel

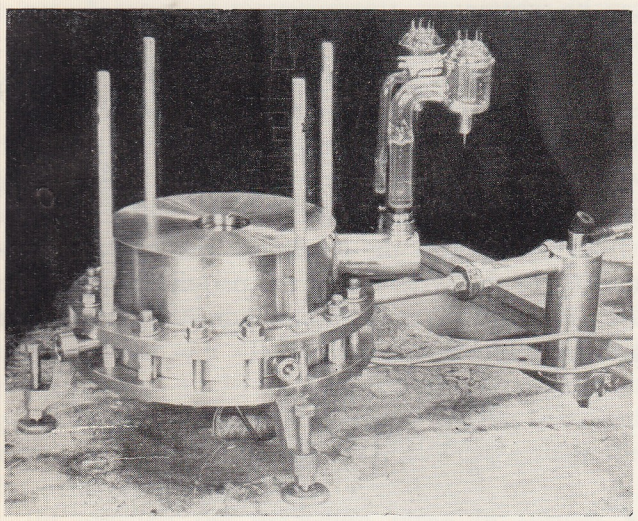

FIG. 4. Photograph of pump prepared for baking.

is about 750°C. In other words, the rotor could be baked while spinning. For bake out, a two section oven floor slips beneath the chamber from either side. then a hood is placed down over the chamber and its associated gauges, sealing the unit.

3. Approximate ultimate pressure calculation

A theoretical pressure ratio has been calculated to evaluate the performance of the pump in the molecular region. The method used to calculate the ultimate pressure ratio is to sum the total mass flow which occurs between the rotor and stator.[8] The total mass flow, as shown in Fig. 5, can be considered as three separate flows: Q_i, the flow induced in the channels of the stator by the motion of the rotor; Q_d, the back diffusive flow in the channels due to the pressure gradient; Q'_d, the radial diffusive flow across the channels through the clearance between the rotor and stator. The ultimate pressure ratio will occur when the mass flow out of the low pressure area equals the mass flow returning by diffusion. Hence at equilibrium:

$$Q_i = Q_d + Q'_d \tag{1}$$

The induced mass flow Q_i through a given cross-sectional area A of the channel is given by: $Q_i = A\bar{v}\varrho g$, where $\bar{v}$ is the induced velocity of the gas molecules along the channel, ϱ the density of the gas and g the number of channels. The induced velocity $\bar{v}$ is equal to the component of velocity of the rotor along the channel times the probability that the molecule comes from the moving surface of the rotor. It is assumed that this probability is the ratio of the area of the moving surface of the channel to the total area of the channel. So $\bar{v}$ can be written:

$$\bar{v} = \omega r \cos\varphi \frac{W}{C} \tag{2}$$

where ω is the angular velocity of the rotor; r the radial distance along the rotor, φ the angle between v_1 and v_T as shown in Fig. 5, W the width of the

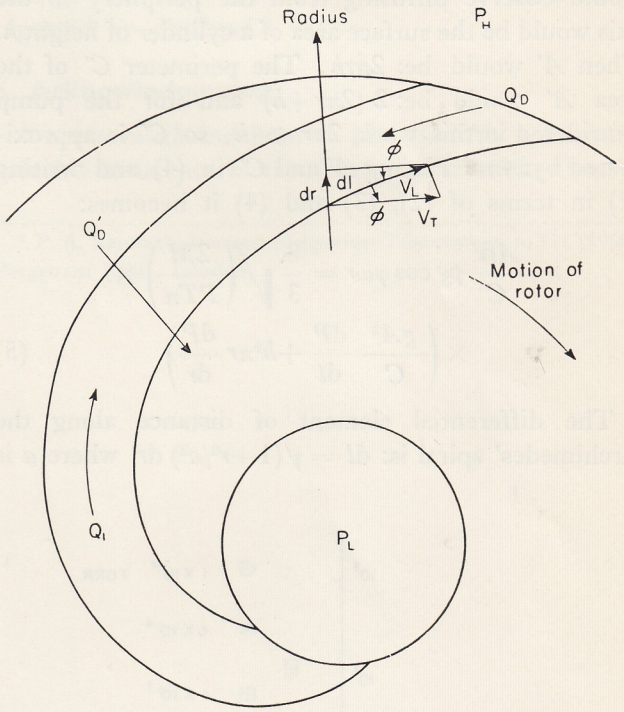

FIG. 5. Mass flow diagram.

channel and C the perimeter of the flow path in the channel. Gas at low density approximates a perfect gas so the expression for the density ϱ can be written in terms of the pressure P and the molecular weight M, ($\varrho = P \times M/RT$). This allows the induced flow Q_i to be expressed as a function of the pressure P and the radial coordinate of the rotor r.

The diffusive flow Q_d is assumed to obey Knudsen's equation for molecular flow. The equation is:

$$Q_d = \frac{8}{3}\sqrt{\left(\frac{2M}{\pi RT}\right)}\frac{A^2}{C}\frac{dP}{dl} \tag{3}$$

[8] R. B. JACOBS, *J. Appl. Phys.* **22**, 217 (1951). S. DUSHMAN, *Vacuum Technique*, p. 151, Wiley, New York (1948).

where dP/dl is the pressure gradient along the channel.

There is a diffusive flow across the channels and this flow is assumed to obey the same Knudsen type equation as (3). This mass flow occurs because of the pressure difference between the axis and periphery. It is:

$$Q'_d = \frac{8}{3}\sqrt{\left(\frac{2M}{\pi RT}\right)}\frac{A'^2}{C'}\frac{dP}{dr} \tag{4}$$

where dP/dr is the pressure gradient along the radius. To evaluate A' and C' in terms of the radius r and the rotor-stator clearance h, consider the parallel surface of the rotor and stator as shown in Fig. 1. The cross-sectional area A' that a molecule of gas would observe diffusing from the periphery to the axis would be the surface area of a cylinder of height h. Then A' would be: $2\pi rh$. The perimeter C' of the area A' would be: $2(2\pi r+h)$ and for the pump considered in this work, $2\pi r \gg h$, so C' is approximated by: $4\pi r$. Placing A' and C' in (4) and writing (1) in terms of (2), (3) and (4) it becomes:

$$\frac{AW}{C}\rho g\cos\varphi\omega r = \frac{8}{3}\sqrt{\left(\frac{2M}{RT\pi}\right)}\times \times\left(\frac{gA^2}{C}\frac{dP}{dl}+h^2\pi r\frac{dP}{dr}\right) \tag{5}$$

The differential element of distance along the Archimedes' spiral is: $dl = \sqrt{(1+r^2/a^2)}\,dr$, where a is the polar subnormal of the spiral. This allows dP/dl to be expressed in terms of dP/dr. Also, with the aid of Fig. 5: $\sin\varphi = dr/dl$, so the cosine term in (5) can be expressed in terms of dr/dl. Now (5) can be written:

$$\alpha\frac{r^2}{a}P = \left[\beta\left(1+\frac{r^2}{a^2}\right)^{-\frac{1}{2}}+r\right]\frac{dP}{dr} \tag{6}$$

where $\alpha = \frac{3}{8}\sqrt{\left(\frac{M}{2\pi RT}\right)}\frac{AW}{Ch^2}g\omega$ and $\beta = \frac{gA^2}{C\pi h^2}$

Solving (6) with the conditions that the forepressure P_H of the system is at the periphery r_1 and the low pressure P_L is at the inside radius r_2, the ultimate pressure ratio is then:

$$\frac{P_H}{P_L} = \exp\left(\int_{r_2}^{r_1}\frac{\alpha dr}{\beta a/r^2+1+a^2/r^2}\right)$$

4. Data and results

The numerical results of the experiments are shown in Fig. 6. The data relates the ultimate pressure ratio to the frequency of the rotor in c/s. It is for a fixed rotor-stator separation of 0.05 cm. The experiments reported were conducted with the residual gases remaining in the chamber after the forepressure system reduced the chamber air pressure from atmospheric to the ultimate low level.

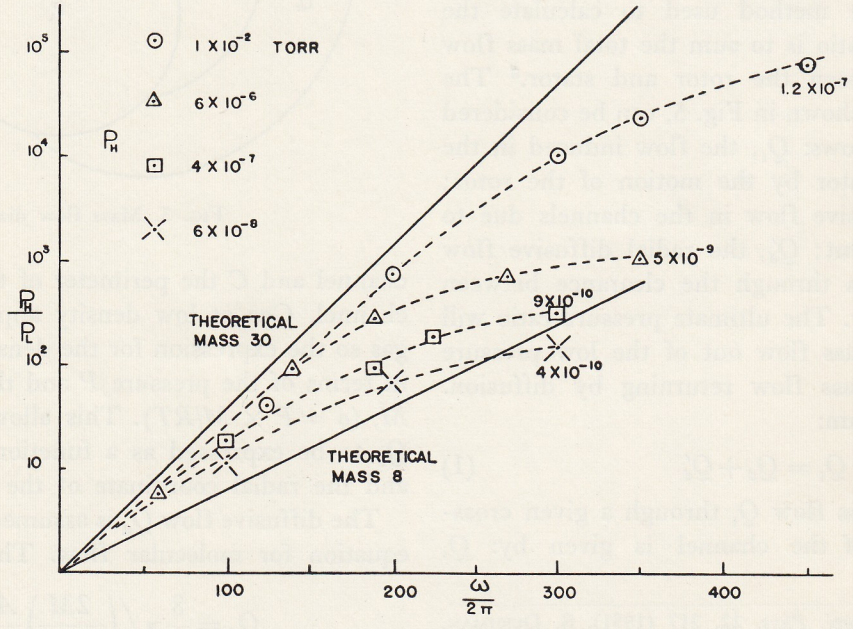

FIG. 6. Comparison of data for various forepressures.

The data showing the maximum pressure ratio recorded to date was with a forepressure of 10^{-2} Torr, a low pressure of 1.2×10^{-7} Torr was measured. This corresponds to a peripherical velocity of 330 m/sec. A series of measurements was made during this run in the 10^{-6} Torr region to obtain a rough pumping speed. It was done by decreasing the rotor-stator separation, then recording the pressure differences and drop times. This gave a speed of 6 to 10 l./sec. When data was recorded with a forepressure of 6×10^{-6} Torr, a low pressure of 5×10^{-9} Torr was measured at a rotor frequency of 350 c/s. Further reducing the forepressure to 4×10^{-7} Torr a pressure ratio of over 400 was measured at 300 c/s. This gave a low pressure of 9×10^{-10} Torr. The lowest measured pressure was 4×10^{-10} Torr where the ionization gauge became completely unreliable. It was measured when the frequency of the rotor was 300 c/s and the forepressure 6×10^{-8} Torr.

By utilizing the procedure given in section 3, one can calculate an ultimate pressure ratio. It was assumed for this calculation that the gas in the system was an ideal gas and had a molecular weight of 30 and a temperature of 300°K. The results of the calculation for a rotor-stator separation of 0.05 cm are shown in Fig. 6 as a solid line labeled Theoretical-Mass 30. This theoretical curve as well as the data are very dependent on the clearance. The calculation and the data agree well at the highest forepressure. However, as the forepressure is lowered the agreement is not as good. There are two reasons for this deviation: the limitations of the ionization gauge employed to measure the pressure, and the questionable validity of the assumption that the residual gas in the system at these lower forepressures has the molecular weight of air. The solid line in Fig. 6, labeled as Theoretical-Mass 8, shows the pressure ratio as a function of rotor frequency when the residual gases are assumed to have an average molecular weight of 8 which is about the average value reported by Redhead.[9]

5. Acknowledgement

We are much indebted to Mr. Earl T. Kinzer for valuable assistance in the development of the theory.

[9] P. A. Redhead, *Vacuum Symposium Transactions*, p. 111 (1960) Pergamon Press, London.